



Article

Epitope Mapping Immunoassay Analysis of the Interaction between β -Amyloid and Fibrinogen

Vo Van Giau and Seong Soo A. An *

Department of Bionano Technology, Gachon University, Seongnam, 1342 Sungnamdaero, Sujeong-Gu, Seongnam, Gyeonggi 461-701, Korea; giauvvo@gmail.com or giauvvo@gachon.ac.kr

* Correspondence: seongaan@gachon.ac.kr or seong.an@gmail.com; Tel./Fax: +82-31-750-8755

Received: 27 December 2018; Accepted: 21 January 2019; Published: 24 January 2019



Abstract: The vast majority of patients with Alzheimer's disease (AD) suffer from impaired cerebral circulation. Substantial evidence indicates that fibrinogen (Fbg) and fibrin clot formation play an important role in this circulatory dysfunction in AD. Fbg interacts with β -amyloid (1-42) ($A\beta$), forming plasmin-resistant abnormal blood clots, and increased fibrin deposition has been discovered in the brains of AD patients and mouse models. In this study, biochemical approaches and the epitope mapping immunoassay were employed to characterize binding epitopes within the Fbg and complementary epitopes in $A\beta$. We discovered the $A\beta$ 5–25 peptide as the most critical region for the interaction, which can be inhibited by specific monoclonal and polyclonal antibodies against the central region of $A\beta$. $A\beta$ binding to Fbg may block plasmin-mediated fibrin cleavage at this site, resulting in the generation of increased levels of plasmin-resistant fibrin degradation fragments. Our study elucidates the $A\beta$ -Fbg interaction that may involve the mechanism by which $A\beta$ -Fbg binding delays fibrinolysis by plasmin, providing valuable information in the development of therapeutic approaches for AD.

Keywords: Alzheimer's disease; amyloid- β ; epitope mapping; ligand; fibrinogen

1. Introduction

Alzheimer's disease (AD) is a neurodegenerative disease in which vascular pathology plays a vital role [1–4]. The most important and well-known pathological features of AD are extracellular β -amyloid (1–42) ($A\beta$) plaques, intracellular tau tangles, neuroinflammation, and neuronal loss [5]. Fibrinogen (Fbg) is a large glycoprotein, composed of two fragment D domains and one fragment E domain, which consist of a heterodimer composed of pairs of α , β , and γ chains [6]. There are several functional consequences of binding of $A\beta$ to Fbg, which induces a structural change in the C-terminal region of the Fbg β -chain (β 384–393) [7] and results in the formation of fibrin with increased resistance to fibrinolysis [7,8]. Accumulating evidence implicates Fbg, the main protein component of blood clots, in the pathogenesis of AD. Hence, disturbances to fibrinolysis may have significant consequences for occlusive and inflammatory pathology in various diseases [3] including AD [9]. Indeed, many studies suggested that the interaction between Fbg and $A\beta$ resulted in forming plasmin-resistant abnormal blood clots, which may be increased fibrin deposition in the brains of AD patients and mouse models [8,10–12]. Fibrin clots can contribute to the pathology of AD by forming occlude capillaries and restricting blood flow. Furthermore, previous studies demonstrated that the $A\beta$ was a factor capable of modulating fibrin clot structure and stability [7,13]. $A\beta$ 42 bound Fbg with a K_d of 26.3 ± 6.7 nM, as well as fibrin clots formed in the presence of $A\beta$ 42, are structurally altered and more resistant to fibrinolysis. $A\beta$ 42 can also bind to pre-formed fibrin and block the access of plasmin to fibrin [7]. Over time, this could lead to disruption of microinfarcts and the blood–brain barrier, which

are pathologies commonly observed in AD. To improve selectivity and potency of therapeutics against the A β -Fbg interaction, a better understanding of their interaction is needed.

In the present study, we discovered the regions within A β responsible for A β -Fbg binding using biochemical approaches and the epitope-mapping enzyme-linked immunosorbent assay (ELISA).

2. Results

2.1. The Preparation of Fbg and A β 42 EpiMap ELISA Tests

The EpiMap ELISA was prepared from an array of synthetic peptides on 96-well microtiter plates using 14 overlapping peptides (15 mer) from the N- to C-terminus of the A β 42 sequence (Figure 5). Overlapping peptides were synthesized with a cysteine residue at the N- or C-terminal ends to conjugate on the maleimide-activated microplates through their free sulfhydryl group. Increased hydrophobicity of overlapping peptides was encouraged with the addition of a cysteine. Unfortunately, the A β peptide no. 15 could not be purified due to its aggregation upon release from the solid-phase peptide synthesis beads. The overlapping peptides were conjugated to a maleimide-activated microplate through a cysteine residue. A schematic explanation of the overlapping peptide conjugation as well as the basic principle of the EpiMap ELISA test is described in Figure 6.

2.2. The Evaluation of Specificity and Sensitivity of the Antibodies

The specificity and sensitivity of the antibodies used in this study, polyclonal rabbit anti-Fbg (pAb) and monoclonal anti-Fbg 85D4 (mAb), were checked with the indirect ELISA system. The pAb had an affinity to Fbg including its fragments D and E, while mAb, capturing only a specific conformational epitope in Fbg fragment D, only had an affinity for Fbg fragment D. Interestingly, Fbg itself showed little binding with mAb even though it contained the Fbg fragment D detected by mAb (Figure 1). Previous results show that the interaction between A β 42 and Fbg or fragment D promotes A β 42 fibrillization [13,14], which may account for the conversion of the oligomeric species of A β 42 seen when incubated alone into fibrils in the presence of fragment D.

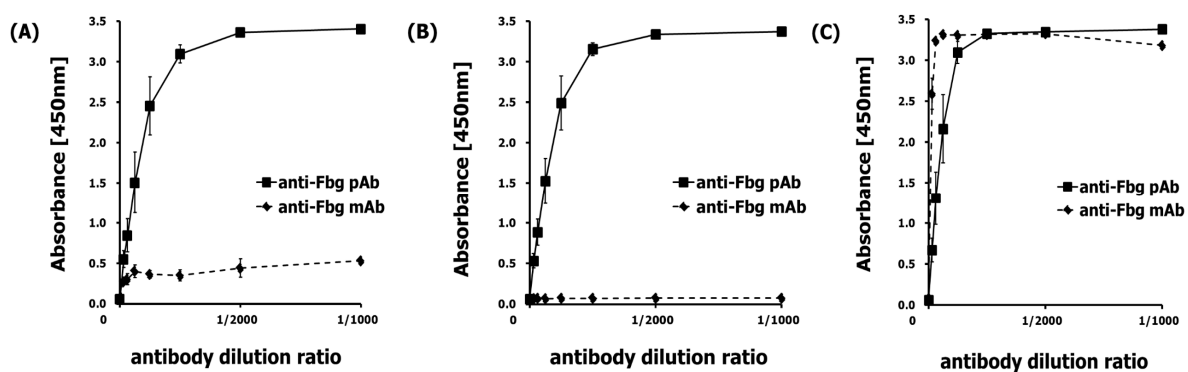


Figure 1. Each anti-Fbg, pAb and mAb, was tested using the indirect ELISA system. (A) At an Fbg-coated plate, the pAb had good affinity while the mAb had poor affinity. (B) At an Fbg fragment E-coated plate, the pAb had good affinity while the mAb had no affinity. (C) At an Fbg fragment D-coated plate, both the pAb and the mAb had good affinity.

2.3. Protein Epitope Mapping with the EpiMap ELISA

Our ELISA-based protein interaction assay was designed to investigate the interaction between Fbg and A β . Binding of Fbg at A β -coated plates was detected by both the pAb and the mAb. Fbg (340 kDa) is composed of 2 sets of 3 polypeptide chains (A α : 67 kDa, B β : 52 kDa, γ : 46.5 kDa), its fragment E (~50 kDa) is composed of truncated small chains (E α : 11 kDa, E β : 14 kDa, E γ : 7 kDa), and its fragment D (85 kDa) is composed of truncated longer chains (D α : 12 kDa, D β : 37.6 kDa, D γ : 41 kDa). All three complexes were identified by a published gel electrophoretic method [15] (Figure 2A).

At 500 $\mu\text{g}/\text{mL}$ in 100 mM carbonate–bicarbonate buffer, the $\text{A}\beta$ stock solution was composed of monomers (4 kDa), oligomers (8–16 kDa), and fibrils (approximately >70 kDa) (Figure 2B). Although a high-concentration solution of $\text{A}\beta$ was used for electrophoresis due to the high detection limit of that assay, the $\text{A}\beta$ used to coat ELISA plates had been diluted to 2 $\mu\text{g}/\text{mL}$ in the carbonate–bicarbonate buffer, which would have lowered the degree of polymerization. The pAb interacted with Fbg and Fbg fragment D in proportion to their concentrations, while rarely interacting with Fbg fragment E even at high concentrations (Figure 2C). Similar to the pAb, the mAb interacted with both Fbg and Fbg fragment D in proportion to their concentrations, while no interaction between the mAb and Fbg fragment E could be detected (Figure 2D). These findings are similar to previous studies [13,14] that found Ab42 binding to fibrin(ogen) delays fibrinolysis by interfering with the binding of plasminogen and plasmin to fibrin [7] and that Ab42 binds to the β -chain of Fbg fragment D.

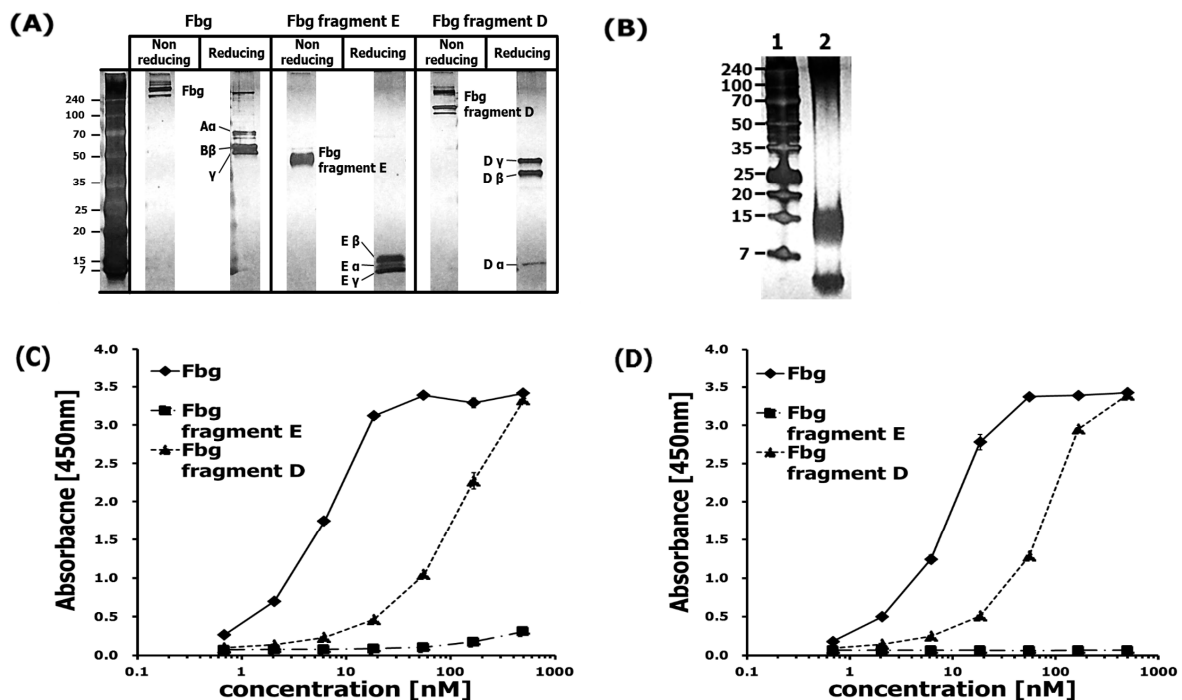


Figure 2. $\text{A}\beta$ 42 binds to Fbg and its fragments. (A) Tris-tricine gel electrophoresis result for Fbg and its fragments D and E. (B) Tris-tricine gel electrophoresis result for: (1) protein marker, and (2) $\text{A}\beta$ 42. (C) Binding of Fbg and its fragments was detected by the pAb. (D) Binding of Fbg and its fragments was detected by the mAb.

To further characterize the differential effect of the Fbg and Fbg-GPRP to the binding of the epitope versus the monoclonal and polyclonal antibodies, indirect ELISA was performed. Figure 3 shows that there was not a significant difference in the use of these two antibodies to detect the binding of Fbg and Fbg-GPRP peptide on $\text{A}\beta$ 42. This interaction study provided additional confirmation of the ELISA study, indicating that either pAb or mAb could have an affinity to the Fbg and Fbg-GPRP.

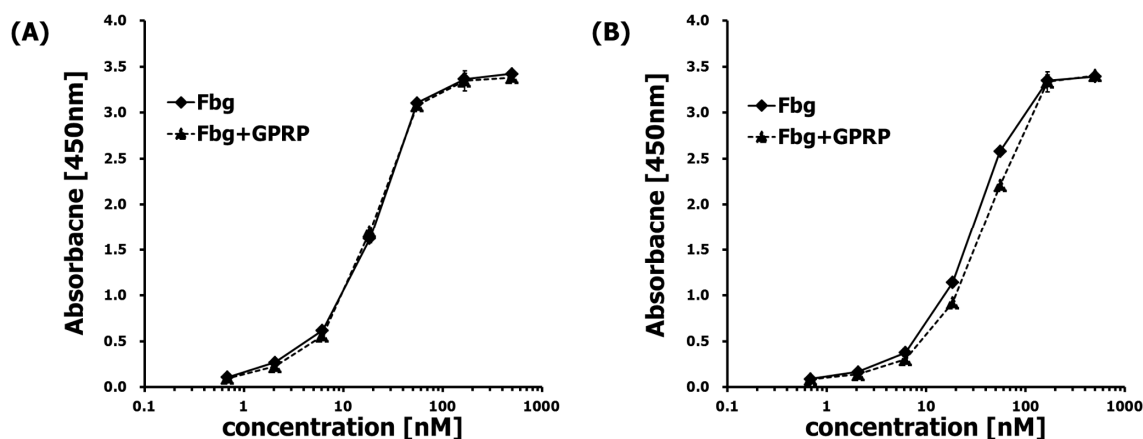


Figure 3. A β 42 binds to Fbg and Fbg-GPRP peptide (1:50 molar ratio). (A) detecting by polyclonal rabbit anti-Fbg and (B) monoclonal anti-Fbg 85D4.

2.4. Fbg Binding Analysis Using A β 42 Epitope-Mapping ELISA

To determine which region of A β 42 is responsible for Fbg binding, fourteen A β fragments (numbered 1–14) were analyzed for their ability to bind Fbg and its fragments by monoclonal and polyclonal antibodies assay (Figure 4A). Among the 14 fragments, only A β 5–25 showed binding to both pAb (Figure 4B) and mAb (Figure 4C) at N-terminus regions.

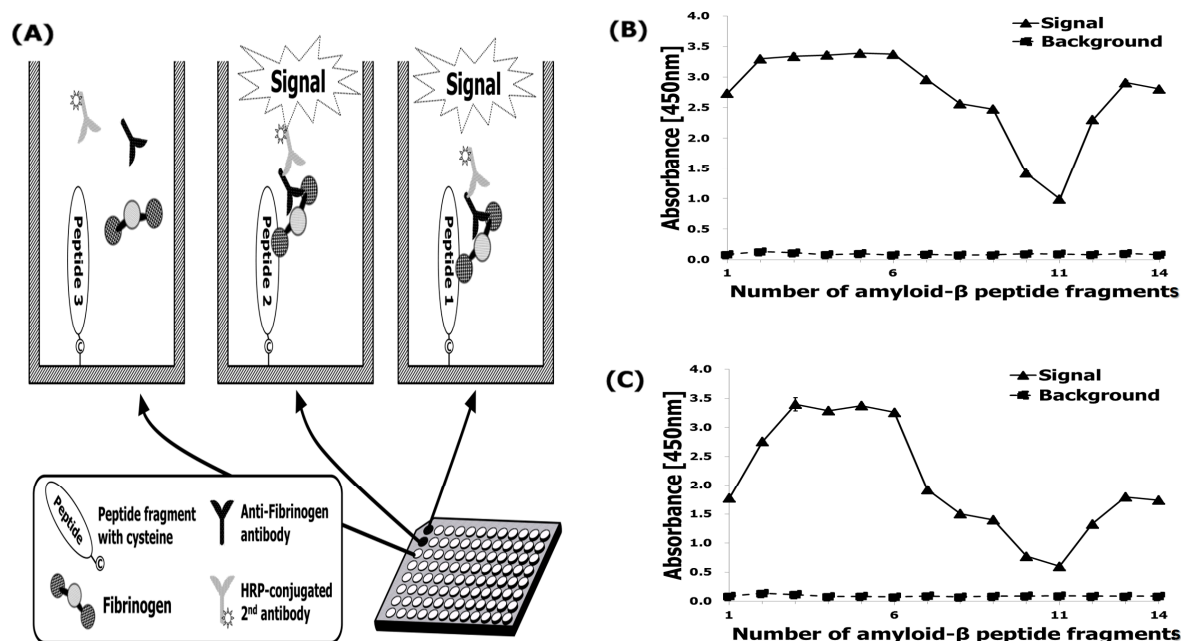


Figure 4. A β 42 epitope-mapping ELISA to find a specific site interacting with Fbg. (A) A β 42 epitope mapping to detect the site of interaction with Fbg. When Fbg bound to a specific sequence in A β 42, the corresponding peptide- Fbg complex was detected by anti- Fbg antibody. (B) Fbg attached to the A β 42 fragments detected by the pAb. (C) Fbg attached to the A β 42 fragments detected by the mAb. Straight line: 100 μ L of 20 μ g/mL Fbg incubated with the antibody for 2 h at 25 $^{\circ}$ C before the Fbg detection step; dotted line: 100 μ L of buffer incubated with the antibody for 2 h at 25 $^{\circ}$ C before the Fbg detection step. The straight line indicates non-specific binding of anti-Fbg antibodies.

However, these figures were recorded with a relatively lower affinity to both fragments with numbering 10 and 11. Meanwhile, an unintended interaction between A β ₄₂ fragments and the anti-Fbg antibodies was not observed. Among the fragments #2 ~ #6, the consensus sequence

corresponded to A β 42 residues 5–25, as presenting Arg-His-Asp-Ser-Gly-Tyr-Glu-Val-His-His-Gln-Lys-Val-Phe-Ala-Glu-Asp-Val-Gly (Figure 5). In both the monoclonal and polyclonal antibodies, all 19 amino acid residues of the epitope were observed to be essential for the binding, consistent with the high selectivity of the antibodies. In contrast, the A β 42 sequence 21–33, which is the consensus sequence for fragments #10 and #11, revealed relatively low affinity for Fbg (Figure 4C), which may be due to a loss of affinity of the fragments for those binding sites [14].

3. Discussion

A β associates with Fbg in vivo and in vitro, which alters the structure of the fibrin clot that is formed [8,10–12]. Since this interaction may have implications for AD pathogenesis, it is critical to gain a better understanding of the biochemical details. In addition, it will be important to which residues of A β are involved in this interaction by analyzing the binding of Fbg to regions of the A β peptide. We examined the Fbg-binding region within A β 42 using an epitope mapping immunoassay analysis. Competitive inhibition of the A β –Fbg interaction showed that A β 5–25 (Figure 4) had higher inhibitory efficacy than A β 1–4 and A β 26–42, suggesting that the peptide may play a physiological role in modulating A β 42-mediated effects on fibrin clots. Previously, A β 17–42 exhibits enhanced aggregation relative to full-length [14], which may be another beneficial consequence of enhancing a-secretase activity as a therapeutic strategy for AD A β 42 [16]. Additionally, our evidence suggests that the A β –Fbg interaction might proceed by a new mechanism independent of the known Fbg knob-hole interaction. These previous findings supported a basis for the present study, which was focused on the identification of the essential amino acids within the A β 4–10 [17] and A β 17–40 [14] and A β 17–42 [14] epitope sequences, and on the evaluation of their relative contribution to the interaction with A β -specific mono- and polyclonal antibodies [18].

One possible explanation for this is that although the N-terminus of A β 42 may be directly involved in the interaction between A β 42 and Fbg, the N-terminal residues of A β 5–25 increase the stability of A β 's tertiary structure and promote its oligomerization, which may promote A β –Fbg binding to the A β fragment with strong affinity to Fbg. Overall, our results suggest that Fbg interacts with the central region of tertiary structured A β 42, which is stabilized by its N-terminal residues. Our results also suggest that targeting the stable of A β 42 via its fragment of N-terminal at 5–25 residues may be an alternative strategy for binding A β 42–Fbg binding.

Furthermore, we also demonstrated that Fbg fragment D contributed predominantly to the interaction, whereas fragment E showed little contribution. Using an mAb for Fbg detection, two experiments were conducted, one with and one without A β . In the absence of A β , a lower binding profile of the mAb to Fbg was measured because of the Fbg molecules being in their native conformation, but a higher binding tendency was detected in the presence of A β because A β binding changed the Fbg conformation, resulting in exposure of a preferred conformational epitope for mAb binding. Epitope mapping of A β demonstrated that Fbg possesses a higher binding affinity to the soluble N-terminus of A β . Consistent with this, the A β oligomer, which has the N-termini exposed and the C-termini buried in the center of the structure [19,20], seems to have a close relationship to the pathology of A β –Fbg interaction. Additionally, a fibrin clot formed in the presence of A β had unusual fibrinolysis resistance [8]. A β –Fbg interaction might be the cause of the chronic inflammation seen in AD. Fbg possesses a versatile binding capability [21] and many studies have focused on its interactions. For example, the $\alpha_{IIb}\beta_3$ integrin of platelets [22] and mast cells [23] was able to bind to Fbg.

Moreover, inflammation-related proteins such as toll-like receptor-4 [24], Mac-1 [25], and CD11c/CD18 [26] interact with Fbg. Fbg, having multiple binding sites, might also bind with A β fragments as well, forming a signaling pathway by which A β could, in principle, potentiate inflammatory processes. The interaction of residues 366–414 of the Fbg β chain with A β has been studied, and it is reported that this sequence is located in proximity to the β hole in Fbg fragment D [13]. In addition, it was also reported that at high molar ratio, GPRP peptide can bind to the Fbg β hole [27]. In the present study, the treatment of Fbg with GPRP peptide had little effect on its ability to bind A β (Figure 3), suggesting

that the A β -Fbg interaction is independent of knob-hole interaction. One study suggested that the sequence of Fbg involved in binding to A β inhibits plasmin accessibility, and/or that A β attachment to Fbg leads to tight fibrin clot formation [7]. This binding model would be similar to the interaction between ApoE and Ab₄₂ [28–30], which contributes to its selectivity and high avidity for Ab oligomers and fibrils, including aggregates composed of N-truncated A β variants, without targeting physiologic Ab monomers. A previous study demonstrated that the binding affinity of soluble A β oligomers to Fbg is nearly 10-fold higher than that of A β monomers [31]. These observations are possible clues as to the binding mechanism, but their interpretation is not yet clear. Fbg has previously been proposed as a potential biomarker for diagnosing AD [32]. Consistent with this, high concentrations of Fbg in the blood may lead to cognitive decline in mild-cognitive-impairment patients [33]. Moreover, a hyperhomocysteinemia showing cognitive decline resembling AD pathology was found to be caused by an A β -Fbg-collagen complex [34]. Some of the research on the relationship between Fbg and AD might lead to new therapeutic approaches [5,31,35].

4. Materials and Methods

4.1. Materials

The whole sequence of the human A β 42 peptide and its fragments were synthesized for epitope mapping by Lugen Sci Co., Ltd., Seoul, Korea. A dual-color, broad-range, pre-stained marker (7–240 kDa) was also purchased from Lugen. Fbg from human plasma, monoclonal anti-Fbg 85D4 (mAb), phosphate buffered saline (PBS), PBS containing TWEEN[®]20 (PBST), 3,3',5,5' tetramethylbenzidine (TMB) liquid substrate system for ELISA, ethylenediaminetetraacetic acid (EDTA), L-cysteine, Tris base, and 2-mercaptoethanol were purchased from Sigma–Aldrich. Human Fbg fragment E, Pierce Protein-Free (PBF) blocking buffer, Pierce maleimide-activated plates, goat anti-rabbit IgG (H + L) secondary antibody, HRP conjugate, goat anti-Mouse IgG (H + L) secondary antibody, HRP conjugate, BupH carbonate–bicarbonate buffer, and Nunc-Immuno[™] MaxiSorp[™] Modules (flat bottom, 96-well format) were obtained from Thermo Scientific. Human Fbg fragment D, polyclonal rabbit anti-Fbg (pAb), and Probumin[®] bovine serum albumin (BSA) were purchased from Millipore. Electrophoresis equipment and reagents were purchased from Bio-Rad Laboratories (Hercules, CA, USA).

4.2. The Preparation of the A β 42 Fragments and A β 42 EpiMap ELISA Tests

Fifteen A β 42 fragments for epitope mapping were synthesized as per our previous work [36]. Each fragment was composed of 15 amino acids (Figure 5). The fragments formed a series of sequences, each member of the series being shifted along the A β 42 sequence by an interval of 2 amino acid residues from the previous member. Unfortunately, the peptides numbered 15 failed to be synthesized due to an aggregation problem. These peptides were generated with a cysteine at the end of the N-terminus of the numbered 1–8 and the C-terminus for the peptides 9–14 for linkage to maleimide-activated plates. The interval of 2 amino acids between fragments resulted in a high resolution of the epitope mapping result.

Each high-concentration synthetic A β fragment solution in dimethyl sulfoxide (DMSO) was first diluted in a PBS buffer (pH 4.5) at a 1:1 volume ratio. These solutions were then further diluted to 25 μ g/mL in the PBS buffer (pH 7.2) containing 10 mM EDTA. Each resulting solution was dispensed into Pierce maleimide-activated plates at 100 μ L per well and incubated overnight at 4 °C (Figure 6). After 3 PBST washes, unreacted maleimide groups were blocked by adding 200 μ L of 25 μ g/mL L-cysteine solution in PBS and incubating at 25 °C for 1 h. After 3 PBST washes, 100 μ L of 20 μ g/mL Fbg in PBS + 1% BSA were aliquotted into the wells and incubated at 25 °C for 2 h. After 3 PBST washes, 100 μ L of detection antibody solution (pAb or mAb diluted 1:5000 in PBS + 1% BSA) were added to the wells and incubated at 25 °C for 1 h. After 3 PBST washes, HRP-conjugated secondary antibody was diluted 1:5000 in PBS and was added at 100 μ L per well and incubated at 25 °C for 1 h.

overnight. After 3 PBST washes, the remaining reactivity of the wells was blocked using Pierce Protein-free blocking buffer at 25 °C for 1 h. After 3 more PBST washes, the plates were dried in a vacuum chamber for 2 h. Antibodies pAb from rabbit and mAb from mouse were serially diluted 1:1000, 1:2000, 1:4000, 1:8000, 1:16,000, 1:32,000, and 1:64,000 in PBS + 1% BSA, and 100 μ L of each dilution were aliquotted into the wells. The plates were incubated for 1 h at 25 °C and washed 3 times with PBST. Each HRP-conjugated secondary antibody was diluted 1:5000 in PBS starting with a volume of 100 μ L, then 100 μ L of secondary solution was added to each well and incubated for 1 h at 25 °C. After 3 PBST washes, 100 μ L of TMB substrate was added to each well and incubated at 37 °C for 25 min. The TMB reaction was stopped by adding 50 μ L of 2NH₂SO₄ to each well. Absorbance at 450 nm was measured with a Victor 3 Perkin–Elmer plate reader. Experimental data were reported as the mean \pm S.E.M. of three replicates.

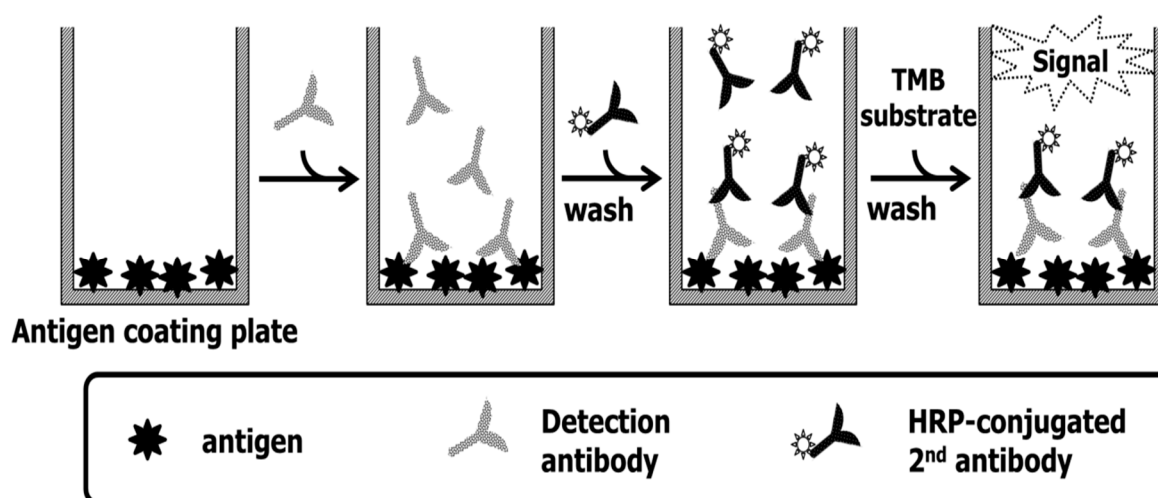


Figure 7. Schematic of indirect ELISA. The antigens were Fbg, Fbg Frag E, and Fbg Frag D. The detection antibodies were pAb and mAb.

4.4. ELISA A β 42–Fbg Interaction Assay

A dilution of 2 μ g/mL in 100 mM carbonate–bicarbonate buffer for 10 mg/mL of A β stock solution in DMSO and 100 μ L/well were dispensed into a Nunc transparent 96-well plate and incubated at 4 °C overnight. After 3 PBST washes, the remaining reactivity of the wells was blocked using Pierce protein-free blocking buffer at 25 °C for 1 h. After 3 PBST washes, the plate was dried in a vacuum chamber for 2 h. Fbg, Fbg fragment E, and Fbg fragment D were each serially diluted 1:1 in PBS + 1% BSA, starting with 0.5 μ M and ending with 7.8125 nM. These protein solutions were dispensed into A β -coated plates at 100 μ L per well and incubated at 25 °C for 2 h. After 3 PBST washes, detection antibody solutions (pAb or mAb diluted 1:5000 in PBS + 1% BSA) were added to the plates at 100 μ L per well and incubated at 25 °C for 1 h. After 3 PBST washes, each well received 100 μ L of HRP-conjugated secondary antibody diluted 1:5000 in PBS followed by incubation at 25 °C for 1 h. After 3 PBST washes, 100 μ L of TMB substrate were aliquotted into each well and incubated at 37 °C for 25 min. The TMB reaction was stopped by adding 50 μ L of 2NH₂SO₄ to the well. Absorbance at 450 nm was measured with a Victor 3 Perkin–Elmer plate reader as described in Figure 8. Experimental data were reported as the mean \pm S.E.M. of three replicates.

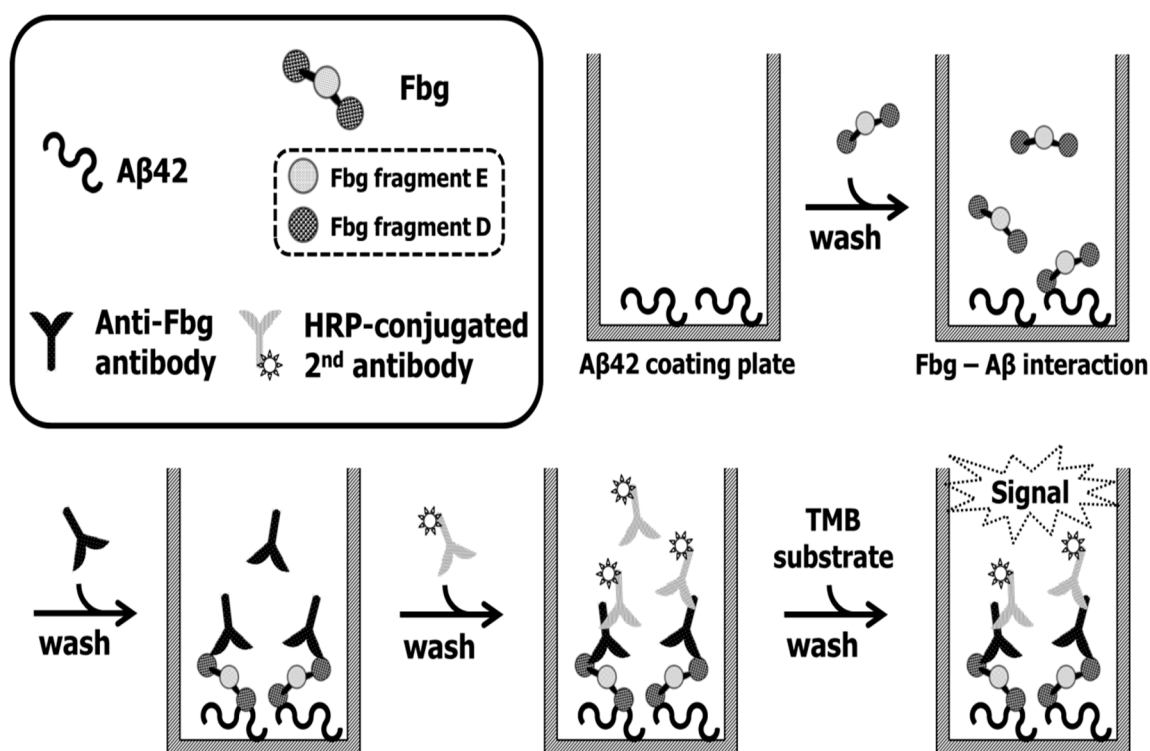


Figure 8. Scheme of the ELISA A β 42-Fbg (fibrinogen) interaction assay.

To explore Fbg binding under conditions of inhibited Fbg polymerization, a 10 mg/mL stock solution of Gly-Pro-Arg-Pro (GPRP) peptide in DMSO was mixed with a 1 mg/mL stock solution of Fbg to produce a 50:1 GPRP:Fbg molar ratio. This solution was serially diluted in PBS + 1% BSA to 1/3 of the previous concentration at each step, starting with 0.5 μ M and ending with 685 pM. These protein solutions were dispensed into A β -coated plates at 100 μ L per well and incubated at 25 $^{\circ}$ C for 2 h. Further processing was the same as above.

4.5. SDS-Stable Complex Formation

Laemmli 4 \times sample buffers with and without 2-mercaptoethanol were prepared according to the manufacturer's instructions (Sigma-Aldrich, St. Louis, MO, USA). Each 500 ng sample of Fbg, Fbg fragment E, or Fbg fragment D was mixed with each sample buffer at a 3:1 volume ratio, heated in boiling water for 3 min, and cooled in an ice bath. A 12% Mini-PROTEAN[®] TGX[™] gel was used for separation and a 1 \times Tris-glycine-SDS running buffer was filled in the gel top and bottom chambers. The samples were loaded, separated slowly, and silver stained.

A β 42 was prepared as a 500 μ g/mL solution in 100 mM carbonate-bicarbonate buffer. After a 4 $^{\circ}$ C overnight incubation, a A β 42 sample was mixed with Tris-tricine sample buffer at a 1:2 volume ratio, heated for 3 min in boiling water, and cooled in an ice bath. A 10–20% Mini-PROTEAN[®] Tris-tricine gel was used for separation. A 1 \times Tris-tricine-SDS cathode buffer was filled in the gel top chamber, and a 0.2 M Tris pH 8.9 buffer was filled in the bottom chamber. The 5 μ g samples were loaded, separated slowly, and silver stained.

5. Conclusions

In conclusion, in the present study, we identified the amino acid residues (A β 5–25) that are critical to the A β -Fbg interaction through specific epitope by monoclonal and polyclonal antibodies. The findings of this study also reveal that antibody epitopes within the center of A β are potentially important for plaque clearance and neuronal protection via an Fbg-mediated mechanism. These results

may contribute the development of effective therapeutics against the A β -Fbg interaction to treat cerebrovascular abnormalities in AD.

Author Contributions: Conceptualization, validation and writing—original draft, V.V.G. and S.S.A.A.; Funding acquisition and supervision, S.S.A.A.

Funding: This research was funded by the National Research Foundation of Korea (NRF) grant by Korean Government NRF-2017R1A2B4012636 and Gachon University Research Grant (2018-0682).

Acknowledgments: The authors gratefully acknowledge the experimental results of MSc. SeunOh Bae from the Department of Bionano Technology.

Conflicts of Interest: The authors declare no conflict of interest.

References

1. Attems, J.; Jellinger, K.A. The overlap between vascular disease and Alzheimer's disease—lessons from pathology. *BMC Med.* **2014**, *12*, 206. [[CrossRef](#)] [[PubMed](#)]
2. Giau, V.V.; Bagyinszky, E.; An, S.S.A.; Kim, S. Clinical genetic strategies for early onset neurodegenerative diseases. *Mol. Cell. Toxicol.* **2018**, *14*, 123–142. [[CrossRef](#)]
3. Giau, V.V.; Wu, S.Y.; Jamerlan, A.; An, S.S.A.; Kim, S.Y.; Hulme, J. Gut Microbiota and Their Neuroinflammatory Implications in Alzheimer's Disease. *Nutrients* **2018**, *10*, 1765. [[CrossRef](#)] [[PubMed](#)]
4. Wang, M.J.; Yi, S.; Han, J.Y.; Park, S.Y.; Jang, J.W.; Chun, I.K.; Giau, V.V.; Bagyinszky, E.; Lim, K.T.; Kang, S.M.; et al. Analysis of Cerebrospinal Fluid and [11C]PIB PET Biomarkers for Alzheimer's Disease with Updated Protocols. *J. Alzheimer's Dis.* **2016**, *52*, 1403–1413. [[CrossRef](#)] [[PubMed](#)]
5. Van Giau, V.; An, S.S.A.; Hulme, J.P. Mitochondrial therapeutic interventions in Alzheimer's disease. *J. Neurol. Sci.* **2018**, *395*, 62–70. [[CrossRef](#)] [[PubMed](#)]
6. Weisel, J.W. Fibrinogen and fibrin. *Adv. Protein Chem.* **2005**, *70*, 247–299. [[PubMed](#)]
7. Zamolodchikov, D.; Strickland, S. Abeta delays fibrin clot lysis by altering fibrin structure and attenuating plasminogen binding to fibrin. *Blood* **2012**, *119*, 3342–3351. [[CrossRef](#)] [[PubMed](#)]
8. Cortes-Canteli, M.; Paul, J.; Norris, E.H.; Bronstein, R.; Ahn, H.J.; Zamolodchikov, D.; Bhuvanendran, S.; Fenz, K.M.; Strickland, S. Fibrinogen and beta-amyloid association alters thrombosis and fibrinolysis: A possible contributing factor to Alzheimer's disease. *Neuron* **2010**, *66*, 695–709. [[CrossRef](#)] [[PubMed](#)]
9. Bagyinszky, E.; Giau, V.V.; Shim, K.; Suk, K.; An, S.S.A.; Kim, S. Role of inflammatory molecules in the Alzheimer's disease progression and diagnosis. *J. Neurol. Sci.* **2017**, *376*, 242–254. [[CrossRef](#)]
10. Cortes-Canteli, M.; Mattei, L.; Richards, A.T.; Norris, E.H.; Strickland, S. Fibrin deposited in the Alzheimer's disease brain promotes neuronal degeneration. *Neurobiol. Aging* **2015**, *36*, 608–617. [[CrossRef](#)]
11. Hultman, K.; Cortes-Canteli, M.; Bounoutas, A.; Richards, A.T.; Strickland, S.; Norris, E.H. Plasmin deficiency leads to fibrin accumulation and a compromised inflammatory response in the mouse brain. *J. Thromb. Haemost.* **2014**, *12*, 701–712. [[CrossRef](#)] [[PubMed](#)]
12. Klohs, J.; Baltés, C.; Princz-Kranz, F.; Ratering, D.; Nitsch, R.M.; Knuesel, I.; Rudin, M. Contrast-enhanced magnetic resonance microangiography reveals remodeling of the cerebral microvasculature in transgenic ArcAbeta mice. *J. Neurosci.* **2012**, *32*, 1705–1713. [[CrossRef](#)] [[PubMed](#)]
13. Ahn, H.J.; Zamolodchikov, D.; Cortes-Canteli, M.; Norris, E.H.; Glickman, J.F.; Strickland, S. Alzheimer's disease peptide beta-amyloid interacts with fibrinogen and induces its oligomerization. *Proc. Natl. Acad. Sci. USA* **2010**, *107*, 21812–21817. [[CrossRef](#)] [[PubMed](#)]
14. Zamolodchikov, D.; Berk-Rauch, H.E.; Oren, D.A.; Stor, D.S.; Singh, P.K.; Kawasaki, M.; Aso, K.; Strickland, S.; Ahn, H.J. Biochemical and structural analysis of the interaction between beta-amyloid and fibrinogen. *Blood* **2016**, *128*, 1144–1151. [[CrossRef](#)]
15. Felding-Habermann, B.; Ruggeri, Z.M.; Cheresh, D.A. Distinct biological consequences of integrin alpha v beta 3-mediated melanoma cell adhesion to fibrinogen and its plasmic fragments. *J. Biol. Chem.* **1992**, *267*, 5070–5077. [[PubMed](#)]
16. Lichtenthaler, S.F. alpha-secretase in Alzheimer's disease: Molecular identity, regulation and therapeutic potential. *J. Neurochem.* **2011**, *116*, 10–21. [[CrossRef](#)]

17. Manea, M.; Przybylski, M.; Hudecz, F.; Mezo, G. Design, structural, and immuno-analytical properties of antigenic bioconjugates comprising a beta-amyloid-plaque specific epitope. *Biopolymers* **2008**, *90*, 94–104. [[CrossRef](#)]
18. Stefanescu, R.; Lupu, L.; Manea, M.; Iacob, R.E.; Przybylski, M. Molecular characterization of the beta-amyloid(4-10) epitope of plaque specific Abeta antibodies by affinity-mass spectrometry using alanine site mutation. *J. Peptide Sci.* **2018**, *24*, e3047. [[CrossRef](#)]
19. Barghorn, S.; Nimmrich, V.; Striebinger, A.; Krantz, C.; Keller, P.; Janson, B.; Bahr, M.; Schmidt, M.; Bitner, R.S.; Harlan, J.; et al. Globular amyloid beta-peptide oligomer—A homogenous and stable neuropathological protein in Alzheimer's disease. *J. Neurochem.* **2005**, *95*, 834–847. [[CrossRef](#)]
20. Ahmed, M.; Davis, J.; Aucoin, D.; Sato, T.; Ahuja, S.; Aimoto, S.; Elliott, J.I.; Van Nostrand, W.E.; Smith, S.O. Structural conversion of neurotoxic amyloid-beta(1-42) oligomers to fibrils. *Nat. Struct. Mol. Biol.* **2010**, *17*, 561–567. [[CrossRef](#)]
21. Davalos, D.; Akassoglou, K. Fibrinogen as a key regulator of inflammation in disease. *Semin. Immunopathol.* **2012**, *34*, 43–62. [[CrossRef](#)] [[PubMed](#)]
22. Holmbäck, K.; Danton, M.J.; Suh, T.T.; Daugherty, C.C.; Degen, J.L. Impaired platelet aggregation and sustained bleeding in mice lacking the fibrinogen motif bound by integrin alpha IIb beta 3. *EMBO J.* **1996**, *15*, 5760–5771. [[CrossRef](#)] [[PubMed](#)]
23. Oki, T.; Kitaura, J.; Eto, K.; Lu, Y.; Maeda-Yamamoto, M.; Inagaki, N.; Nagai, H.; Yamanishi, Y.; Nakajima, H.; Kumagai, H.; et al. Integrin alphaIIb beta3 induces the adhesion and activation of mast cells through interaction with fibrinogen. *J. Immunol.* **2006**, *176*, 52–60. [[CrossRef](#)] [[PubMed](#)]
24. Smiley, S.T.; King, J.A.; Hancock, W.W. Fibrinogen stimulates macrophage chemokine secretion through toll-like receptor 4. *J. Immunol.* **2001**, *167*, 2887–2894. [[CrossRef](#)] [[PubMed](#)]
25. Lishko, V.K.; Podolnikova, N.P.; Yakubenko, V.P.; Yakovlev, S.; Medved, L.; Yadav, S.P.; Ugarova, T.P. Multiple binding sites in fibrinogen for integrin alphaMbeta2 (Mac-1). *J. Biol. Chem.* **2004**, *279*, 44897–44906. [[CrossRef](#)] [[PubMed](#)]
26. Nham, S.U. Characteristics of fibrinogen binding to the domain of CD11c, an alpha subunit of p150,95. *Biochem. Biophys. Res. Commun.* **1999**, *264*, 630–634. [[CrossRef](#)] [[PubMed](#)]
27. Laudano, A.P.; Doolittle, R.F. Studies on synthetic peptides that bind to fibrinogen and prevent fibrin polymerization. Structural requirements, number of binding sites, and species differences. *Biochemistry* **1980**, *19*, 1013–1019. [[CrossRef](#)]
28. Munson, G.W.; Roher, A.E.; Kuo, Y.M.; Gilligan, S.M.; Reardon, C.A.; Getz, G.S.; LaDu, M.J. SDS-stable complex formation between native apolipoprotein E3 and beta-amyloid peptides. *Biochemistry* **2000**, *39*, 16119–16124. [[CrossRef](#)]
29. Giau, V.V.; Bagyinszky, E.; An, S.S.; Kim, S.Y. Role of apolipoprotein E in neurodegenerative diseases. *Neuropsychiatr. Dis. Treat.* **2015**, *11*, 1723–1737. [[CrossRef](#)]
30. Youn, Y.C.; Lim, Y.K.; Han, S.H.; Giau, V.V.; Lee, M.K.; Park, K.Y.; Kim, S.; Bagyinszky, E.; An, S.S.A.; Kim, H.R. Apolipoprotein epsilon7 allele in memory complaints: Insights through protein structure prediction. *Clin. Interv. Aging* **2017**, *12*, 1095–1102. [[CrossRef](#)]
31. Ahn, H.J.; Glickman, J.F.; Poon, K.L.; Zamolodchikov, D.; Jno-Charles, O.C.; Norris, E.H.; Strickland, S. A novel Abeta-fibrinogen interaction inhibitor rescues altered thrombosis and cognitive decline in Alzheimer's disease mice. *J. Exp. Med.* **2014**, *211*, 1049–1062. [[CrossRef](#)] [[PubMed](#)]
32. Lee, J.W.; Namkoong, H.; Kim, H.K.; Kim, S.; Hwang, D.W.; Na, H.R.; Ha, S.-A.; Kim, J.-R.; Kim, J.W. Fibrinogen gamma-A chain precursor in CSF: A candidate biomarker for Alzheimer's disease. *BMC Neurol.* **2007**, *7*, 14. [[CrossRef](#)] [[PubMed](#)]
33. Xu, G.; Zhang, H.; Zhang, S.; Fan, X.; Liu, X. Plasma fibrinogen is associated with cognitive decline and risk for dementia in patients with mild cognitive impairment. *Int. J. Clin. Pract.* **2008**, *62*, 1070–1075. [[CrossRef](#)] [[PubMed](#)]
34. Muradashvili, N.; Tyagi, R.; Metreveli, N.; Tyagi, S.C.; Lominadze, D. Ablation of MMP9 gene ameliorates paracellular permeability and fibrinogen-amyloid beta complex formation during hyperhomocysteinemia. *J. Cereb. Blood Flow Metab.* **2014**, *34*, 1472–1482. [[CrossRef](#)] [[PubMed](#)]

35. Nguyen, T.T.; Giau, V.V.; Vo, T.K. Current advances in transdermal delivery of drugs for Alzheimer's disease. *Indian J. Pharmacol.* **2017**, *49*, 145–154. [[PubMed](#)]
36. Kang, M.; Kim, S.Y.; An, S.S.; Ju, Y.R. Characterizing affinity epitopes between prion protein and beta-amyloid using an epitope mapping immunoassay. *Exp. Mol. Med.* **2013**, *45*, e34. [[CrossRef](#)] [[PubMed](#)]



© 2019 by the authors. Licensee MDPI, Basel, Switzerland. This article is an open access article distributed under the terms and conditions of the Creative Commons Attribution (CC BY) license (<http://creativecommons.org/licenses/by/4.0/>).